DOI: 10.1002/chem.201101250

Retrieving the Most Prevalent Small Fullerene C_{56}

Ting Zhou, Yuan-Zhi Tan, Gui-Juan Shan, Xian-Mei Zou, Cong-Li Gao, Xiang Li, Ke Li, Lin-Long Deng, Rong-Bin Huang, Lan-Sun Zheng, and Su-Yuan Xie*[a]

Owing to the predicted unusual properties and higher curvature on the cages, the fullerenes smaller than C_{60} have attracted much attention in the past 12 years.[1,2] C_{56} is the most prevalent small fullerene, as suggested by the original gas-phase experiments conducted in the mid 1980s.[3] Such a remarkable abundance for C_{56} clusters can be reasonably attributed to the atypical stability of some of the 56-atom fullerene isomers. Theoretical calculations validated that D_2-$^{\#916}C_{56}$, C_s-$^{\#864}C_{56}$, C_{2v}-$^{\#913}C_{56}$, and C_2-$^{\#843}C_{56}$ (the numbers refer to the Fowler–Manolopoulos code[4]) are the four isomers with the lowest energy among a total of 924 topologically possible isomers of C_{56}.[5] Their unavoidable defiance of the isolated pentagon rule (IPR),[6] however, hinders the synthesis of C_{56} in a pure all-carbon form. Non-IPR fullerenes could possibly be stabilized by exohedral or endohedral modification.[7] For non-IPR fullerenes smaller than C_{60}, however, there is no evidence to support the encapsulation of any atom/cluster by the smaller cage in the solid state. Alternatively, small fullerenes, such as C_{20}, $^{\#271}C_{50}$, $^{\#540}C_{54}$, and heptagon-incorporating C_{58},[2b,c,g,8] can be realized by exohedral derivatization. C_{2v}-$^{\#913}C_{56}$ and C_s-$^{\#864}C_{56}$ have recently been exohedrally stabilized as $^{\#913}C_{56}Cl_{10}$[2f] and $^{\#864}C_{56}Cl_{12}$,[2g] respectively, but D_2-symmetric $^{\#916}C_{56}$ with a comparable low energy is still missing. Herein we show such an elusive C_{56} isomer in the form of $^{\#916}C_{56}Cl_{12}$ (Figure 1). It was isolated from the soot of a chlorine-based graphite arc-discharge and identified with X-ray crystallography. The retrieval of $^{\#916}C_{56}$ provides a valuable chance to experimentally explore the most abundant small fullerene C_{56} and, to some extent, is helpful in understanding the prevalence of C_{56} in the clustering process.

The new chloride of C_{56} was produced in the Krätschmer–Huffman[9] arc-discharge reactor with the atmosphere of 0.1974 atm helium and 0.0395 atm CCl_4.[10] Crude soot, produced at a rate of 3 g per hour with an arc-discharge current of approximately 100 A and a voltage of approximately 38 V, was extracted with toluene in a supersonic bath, followed by separation and purification using multistage recycling high-performance liquid chromatography (HPLC) under a temperature of 40 °C (see the Experimental Section for the details). About 2 mg purified sample was obtained after six HPLC runs.

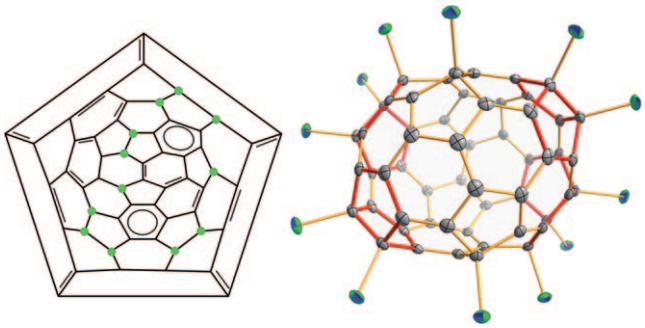

Figure 1. The Schlegel diagram (left) and ORTEP structure (right) of $^{\#916}C_{56}Cl_{12}$ with thermal ellipsoids at 50% probability (the fused pentagons are highlighted in red). The chlorine atoms in the Schlegel diagram are indicated as green dots.

The composition of the purified sample was confirmed by using mass spectrometry (MS) with an atmosphere pressure chemical ionization source. As shown in Figure 2, the isotopic distribution around 1097.7 m/z in the recorded mass spectrum matches well with the simulated $C_{56}Cl_{12}$ pattern. The sequential dechlorination (e.g. ca. 1025.8 m/z) in the spectrum indicates that the $C_{56}Cl_{12}$ molecule is produced from exohedral (rather than endoheral) chlorination on the surface of the C_{56} cage.

By solvent evaporation from its toluene solution, a wine red crystal of $^{\#916}C_{56}Cl_{12}$ was obtained for X-ray crystallo-

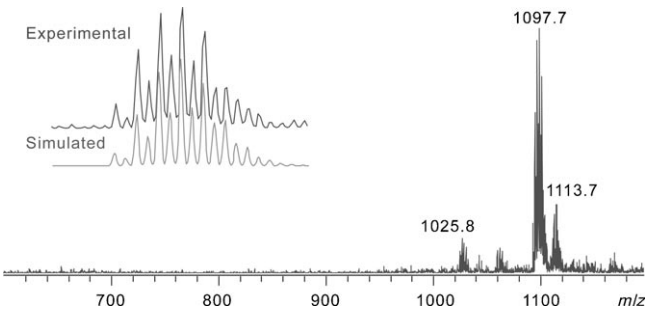

Figure 2. Mass spectra of $^{\#916}C_{56}Cl_{12}$. The insets are the amplified pattern of experimental and simulated molecular ions peaks (ca. 1097.7 m/z). The peaks around 1113.7 might result from the oxidation of $^{\#916}C_{56}Cl_{12}$.

[a] T. Zhou, Y.-Z. Tan, G.-J. Shan, X.-M. Zou, C.-L. Gao, X. Li, K. Li, L.-L. Deng, Prof. R.-B. Huang, Prof. Dr. L.-S. Zheng, Prof. Dr. S.-Y. Xie
State Key Laboratory for Physical Chemistry of Solid Surfaces and Department of Chemistry, College of Chemistry and Chemical Engineering
Xiamen University, Xiamen 361005 (China)
Fax: (+86) 592-2183047
E-mail: syxie@xmu.edu.cn

graphic analysis.[11] It was established that $^{\#916}C_{56}Cl_{12}$ molecules were assembled in a layer-by-layer pattern that mainly depended on the Cl···Cl and C–Cl···π interactions in the crystal. Two toluene molecules were included in each crystal unit cell as well. The geometric structure of $^{\#916}C_{56}Cl_{12}$ with a D_2-symmetric chiral $^{\#916}C_{56}$ fullerene core was unambiguously characterized (Figure 1, the ORTEP structure). There are four pairs of fused pentagons in the $^{\#916}C_{56}$ cage, which is one of the four lowest-energy C_{56} fullerenes (i.e., $^{\#916}C_{56}$, $^{\#843}C_{56}$, as well as the earlier identified $^{\#864}C_{56}$ and $^{\#913}C_{56}$) with minimal fused pentagons among the 924 topologically possible isomers of C_{56}.

By chlorination with D_2-$^{\#916}C_{56}$, the molecular symmetry is lowered to C_2 in $^{\#916}C_{56}Cl_{12}$. Eight chlorine atoms are linked to four pairs of pentagon–pentagon fusions to relieve the fused-pentagon-related strain, while the remaining four chlorine atoms are bonded to the 1,4 positions of two hexagons next to the pentagon–pentagon fusions. The additional four chlorine atoms are necessary for maintaining the aromaticity of the remaining carbon framework. As shown in the Schlegel diagram in Figure 1, the sp^3-hybridized carbon atoms form a band to separate the fullerene cage into two sp^2-hybridized aromatic carbon domains, that is, C_{18} and C_{26}. The bonds associated with these sp^2-hybridized carbon atoms are approximately 1.335–1.481 Å in length, which are in the range of typical C–C/C=C bonds in a fullerene molecule. The C_{18} skeleton is similar to chrysene, while the C_{26} framework is analogous to a $C_{26}H_{12}$ that was named as Yin-Yang fluoranthene by Scott.[12] In agreement with the formerly reported non-IPR chlorofullerenes,[2,13,14] the chlorination pattern of $^{\#916}C_{56}Cl_{12}$ is reasonable and further validates both the strain relief and local aromaticity principles.[7]

The purified sample is moderately soluble in the solvents traditionally used for fullerene research (e.g., carbon disulfide, chloroform, and toluene). The UV/Vis spectrum of $^{\#916}C_{56}Cl_{12}$ in toluene shows broad absorptions at 334, 355, 401, 472, 505, 541, and 587 nm (Figure 3). Interestingly, in comparison with the previously isolated chlorofullerenes $^{\#913}C_{56}Cl_{10}$ and $^{\#864}C_{56}Cl_{12}$, the onset absorption was red-shifted by approximately 74 nm and approximately 111 nm, respectively, implying a cage-dependent optical property. This tunable absorption property, together with the broad absorption (with a molar absorption coefficient of ca. $3.0\times10^2\,L\,mol^{-1}\,cm^{-1}$ even at a wavelength as high as 587 nm) in sunlight might render $^{\#916}C_{56}Cl_{12}$ potentially useful in some advanced technical fields such as fullerene-based solar cells.

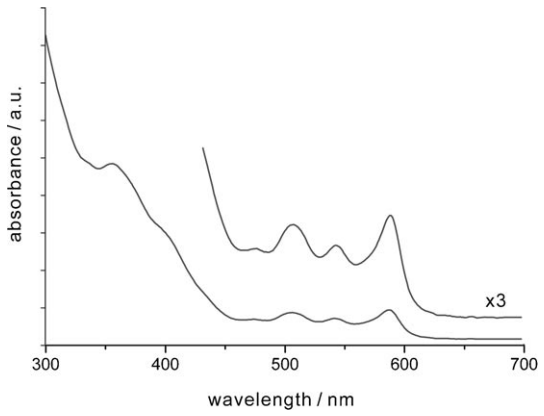

Figure 3. UV/Vis spectrum of $^{\#916}C_{56}Cl_{12}$. The molar absorption coefficient for the absorption at 587 nm is approximately $3.0\times10^2\,L\,mol^{-1}\,cm^{-1}$.

For valuating the potential photovoltaic applications, it is important to know about the electrochemical properties of the involved materials. Accordingly, the cyclic voltammogram (CV) of $^{\#916}C_{56}Cl_{12}$ was recorded at a scan rate of $2\,V\,s^{-1}$ on a Pt electrode in a solution of *o*-dichlorobenzene (*o*-DCB)/acetonitrile (5:1) containing tetrabutylammonium hexafluorophosphate (Bu_4NPF_6) ($0.1\,mol\,L^{-1}$). $^{\#916}C_{56}Cl_{12}$ undergoes a reduction process at −0.79 V. This first reduction potential (−0.79 V vs. Ag/Ag^+ in *o*-DCB/CH_3CN (5:1)) is higher than the corresponding value of C_{60} (−1.07 V vs. Fc/Fc^+ in *o*-DCB),[15–18] likely implying a lower LUMO level for $^{\#916}C_{56}Cl_{12}$ and a lower open circuit voltage for a $^{\#916}C_{56}Cl_{12}$-based organic solar cell. However, it should be noted that a realistic photovoltaic application heavily depends on the macroscopic synthesis of the involved C_{56} material that is still underway at this stage.

In addition to the $^{\#913}C_{56}$ and $^{\#864}C_{56}$ previously reported,[2f,g] $^{\#916}C_{56}$ is the third C_{56} isomer captured from the graphite arc-discharge. The capture of three C_{56} isomers in the same reaction system is intriguing and may provide a much needed starting point for mechanistic studies of fullerene formation. All of them are low-energy C_{56} isomers with relative energies [at B3LYP/6-31G(*d*) level] of 0.0, 0.0, and $7.9\,kcal\,mol^{-1}$ for $^{\#916}C_{56}$, $^{\#864}C_{56}$, and $^{\#913}C_{56}$, respectively (note that the data could be slightly different depending on the calculation methods).[5] The attainability of these multiform low-energy isomers might indicate the formation of fullerene was controlled thermodynamically, and help explain the prevalence of C_{56} species in the clustering process.[3]

It has been commonly suggested that a Stone–Wales (SW) transformation[19] may be involved in the ultimate stage of fullerene formation.[20] Recently, the involvement of the SW transformation has been supported by Troyanov and coworkers through the chlorination of IPR-satisfying $^{\#19150}C_{76}$ with $SbCl_5$ at 340 °C to produce a non-IPR $^{\#18\,917}C_{76}Cl_{24}$[13] experimentally. It may not be entirely unreasonable to assume the existence of such a SW scheme during the formation of C_{56} fullerene, because the three already identified C_{56} isomers can be isomerized from each other by such a SW transformation structurally (Figure 4). As shown in Figure 4, the SW transformation from C_{2v}-$^{\#913}C_{56}$ to C_s-$^{\#864}C_{56}$ and from C_s-$^{\#864}C_{56}$ to D_2-$^{\#916}C_{56}$ each involves only one 90° rotation of C–C bond between two abutting hexagons. However, hard and unambiguous experimental evidence supporting such a pathway for C_{56} isomer has yet to be obtained.

To conclude, D_2-symmetric C_{56}, in addition to the other two reported isomers (C_{2v}-$^{\#913}C_{56}$ and C_s-$^{\#864}C_{56}$), was stabilized as $^{\#916}C_{56}Cl_{12}$ in the chlorine-based arc-discharge of graphite. Its geometric structure with four pairs of fused pentagons has been unambiguously identified by single-crystal X-ray crystallography. The chlorination pattern of

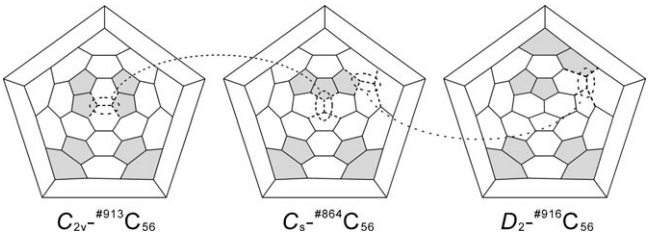

Figure 4. The Schlegel diagrams of $^{\#913}C_{56}$, $^{\#864}C_{56}$, and $^{\#916}C_{56}$. The bonds involved in the SW transformation from $^{\#913}C_{56}$ to $^{\#864}C_{56}$ and finally to $^{\#916}C_{56}$ are denoted by the dash lines and circles.

$^{\#916}C_{56}Cl_{12}$ is in agreement with both the strain relief and the local aromaticity principles that facilitate the stabilization of $^{\#916}C_{56}Cl_{12}$. The attainability of this novel $^{\#916}C_{56}$ renders the C_{56} family as the first fullerene family having three non-IPR isomers experimentally available and provides valuable material to study the potential properties of the most prevalent small fullerene. Based on the available UV/Vis spectra of the three C_{56} species, for example, a cage-dependent optical property is shown for the chlorides of C_{56} isomers. In terms of the structure, the newly identified $^{\#916}C_{56}$ can be obtained from the formerly reported C_{2v}-$^{\#913}C_{56}$ and C_s-$^{\#864}C_{56}$ by SW transformation, thus contributing to the study of the mechanism responsible for fullerene formation.

Experimental Section

The soot containing $^{\#916}C_{56}Cl_{12}$ was produced under 0.1974 atm helium and 0.0395 atm CCl_4 in a modified Krätschmer–Huffman arc-discharge reactor.[9,10] A toluene-extract sample was extracted by using toluene in an ultrasonic bath, and was then purified by multistep HPLC separation on a SHIMADZU prep-HPLC instrument. The HPLC procedure involved six HPLC runs, among which the last one was carried out under a recycling mode. All the separations were performed at room temperature, with toluene as eluent. The crude toluene-extract of soot was initially separated by using a pyrenebutyric acid bonded silica column (I.D. 20×250 mm) at a flow rate of 10 mL min^{-1}, and the components with a retention time ranging from 7.0 to 10.5 min were collected for subsequent separation. In the second HPLC stage, the collected components were separated by a Buckyprep column (I.D. 10×250 mm) at a flow rate of 6 mL min^{-1}, and then the components with a retention time ranging from 13.0 to 18.5 min were collected. Then a Buckyprep-M column (I.D. 10×250 mm) was employed to conduct the separation at a flow rate of 2.5 mL min^{-1} with the components ranging from 10.6 to 13.5 min collected. Again the Buckyprep-M column (I.D. 10×250 mm) was used to carry out the fourth run of separation with a flow rate of 4 mL min^{-1} and the components with a retention time from 7.8 to 9.3 min were collected. During the fifth separation run, the sample with $C_{56}Cl_{12}$ was collected after separation on a Buckyprep column (I.D. 10×250 mm) at a flow rate of 4 mL min^{-1}. In the last stage, the collected sample from the fifth run was purified in a recycling HPLC mode on the same Buckyprep column (I.D. 10×250 mm) with the same flow rate of 4 mL min^{-1}. After four separation cycles in the last stage, the HPLC chromatogram shows a sharp peak corresponding to the purified $^{\#916}C_{56}Cl_{12}$. About 2 mg of $^{\#916}C_{56}Cl_{12}$ with high purity was isolated from the toluene-soluble soot. Evaporation of the toluene solution afforded wine red single crystals of $^{\#916}C_{56}Cl_{12}$. X-ray diffraction data were collected on a Rigaku diffractometer ($Mo_{K\alpha}$ radiation (0.71073 Å), graphite monochromator). The structure was solved and refined by using SHELXL-97.[21] The mass spectrometry of $^{\#916}C_{56}Cl_{12}$ was conducted on a Bruker Esquire HCT mass spectrometer with an atmospheric pressure chemical ionization (APCI) ion source in the negative-ion mode. The dry gas temperature was set at 250 °C, and the APCI temperature was at 300 °C. The UV/Vis spectrum of $C_{56}Cl_{12}$ was recorded on a THERMO Evolution 300 UV/Visible spectrophotometer.

The electrochemical measurements were performed by using a CHI-660C analyzer (CH Instruments, Inc.) in a glove box at room temperature (20 ± 2 °C) under a nitrogen atmosphere. A conventional three-electrode cell was used, with a Pt disk, a Pt wire, and an Ag/Ag^+ electrode ($AgNO_3$ (0.01 mol L^{-1}), Bu_4NPF_6 (0.09 mol L^{-1}) in acetonitrile) as working electrode, counter electrode, and reference electrode, respectively, in a Bu_4NPF_6 (0.1 mol L^{-1}), *o*-DCB/CH_3CN (5:1) solution. All potentials were reported versus the redox couple of an internal Ag/Ag^+ standard. Before measurement, the working electrodes were polished with alumina slurry (0.3 μm), and subsequently ultrasonicated in doubly distilled water, followed by drying in nitrogen atmosphere.

Acknowledgements

The authors thank Professor Yu-Qi Feng from Wuhan University for the HPLC support. This work was supported by the NNSF of China (grant numbers 20721001, 21031004) and the 973 Program (grant numbers 2007CB815301 and 2011CB935901).

Keywords: C_{56} · cage compounds · fullerenes · isolated-pentagon-rule · X-ray diffraction

[1] X. Lu, Z. F. Chen, *Chem. Rev.* **2005**, *105*, 3643–3696, and references therein.

[2] a) C. Piskoti, J. Yarger, A. Zettl, *Nature* **1998**, *393*, 771–774; b) S. Y. Xie, F. Gao, X. Lu, R. B. Huang, C. R. Wang, X. Zhang, M. L. Liu, S. L. Deng, L. S. Zheng, *Science* **2004**, *304*, 699–699; c) P. A. Troshin, A. G. Avent, A. D. Darwish, N. Martsinovich, A. K. Abdul-Sada, J. M. Street, R. Taylor, *Science* **2005**, *309*, 278–281; d) E. Sackers, T. Obwald, K. Weber, M. Keller, D. Hunkler, J. Worth, L. Knothe, H. Prinzbach, *Chem. Eur. J.* **2006**, *12*, 6242–6254; e) F. Wahl, A. Weiler, P. Landenberger, E. Sackers, T. Voss, A. Haas, M. Lieb, D. Hunkler, J. Worth, L. Knothe, H. Prinzbach, *Chem. Eur. J.* **2006**, *12*, 6255–6267; f) Y. Z. Tan, X. Han, X. Wu, Y. Y. Meng, F. Zhu, Z. Z. Qian, Z. J. Liao, M. H. Chen, X. Lu, S. Y. Xie, R. B. Huang, L. S. Zheng, *J. Am. Chem. Soc.* **2008**, *130*, 15240–15241; g) Y. Z. Tan, J. Li, F. Zhu, X. Han, W. S. Jiang, R. B. Huang, Z. Zheng, Z. Z. Qian, R. T. Chen, Z. J. Liao, S. Y. Xie, X. Lu, L. S. Zheng, *Nat. Chem.* **2010**, *2*, 269–273.

[3] a) E. A. Rohlfing, D. M. Cox, A. Kaldor, *J. Chem. Phys.* **1984**, *81*, 3322–3330; b) H. W. Kroto, J. R. Heath, S. C. O' Brein, R. F. Curl, R. E. Smalley, *Nature* **1985**, *318*, 162–163.

[4] P. W. Fowler, D. E. Manolopoulos, *An Atlas of Fullerenes*, Clarendon Press, Oxford, **1995**.

[5] a) P. Celani, H. J. Werner, *J. Chem. Phys.* **2000**, *112*, 5546–5557; b) S. Diaz-Tendero, F. Martin, M. Alcami, *Comput. Mater. Sci.* **2006**, *35*, 203–209; c) N. Shao, Y. Gao, X. C. Zeng, *J. Phys. Chem. C.* **2007**, *111*, 17671–17677; d) D. L. Chen, W. Q. Tian, J. K. Feng, C. C. Sun, *J. Chem. Phys.* **2008**, *128*, 044318.

[6] H. W. Kroto, *Nature* **1987**, *329*, 529–531.

[7] Y. Z. Tan, S. Y. Xie, R. B. Huang, L. S. Zheng, *Nat. Chem.* **2009**, *1*, 450–460.

[8] a) R. J. Ternansky, D. W. Balogh, L. A. Paquette, *J. Am. Chem. Soc.* **1982**, *104*, 4503–4504; b) L. A. Paquette, R. J. Ternansky, D. W. Balogh, *J. Am. Chem. Soc.* **1982**, *104*, 4502–4503.

[9] W. Krätschmer, L. D. Lamb, K. Fostiropoulos, D. R. Huffman, *Nature* **1990**, *347*, 354–358.

[10] F. Gao, S. Y. Xie, R. B. Huang, L. S. Zheng, *Chem. Commun.* **2003**, 2676–2677.

[11] Crystal data for C_2-symmetric $C_{56}Cl_{12}$ (#916): wine red crystal ($0.15\times0.10\times0.08$ mm^3); triclinic; space group $P\bar{1}$; $a=11.1464(10)$, $b=$

12.9379(14), c=16.7216(13) Å; α =68.497(9), β =78.893(7), γ =70.374(9)°; V=2106.6(3) Å^3; Z=2; T=173(2) K; R_1=0.0401, wR_1=0.0953 [$F_o > 2\sigma$ (F_o)]; R_2=0.0496, wR_2=0.1004 (all data). CCDC 812184 contains the supplementary crystallographic data for this paper. These data can be obtained free of charge from The Cambridge Crystallographic Data Centre via www.ccdc.cam.ac.uk/data_request/cif.

[12] V. M. Tsefrikas, L. T. Scott, *Chem. Rev.* **2006**, *106*, 4868–4884.

[13] I. N. Ioffe, A. A. Goryunkov, N. B. Tamm, L. N. Sidorov, E. Kemnitz, S. I. Troyanov, *Angew. Chem.* **2009**, *121*, 6018–6021; *Angew. Chem. Int. Ed.* **2009**, *48*, 5904–5907.

[14] a) K. Ziegler, A. Mueller, K. Y. Amsharov, M. Jansen, *J. Am. Chem. Soc.* **2010**, *132*, 17099–17101; b) Y. Z. Tan, T. Zhou, J. Bao, G. J. Shan, S. Y. Xie, R. B. Huang, L. S. Zheng, *J. Am. Chem. Soc.* **2010**, *132*, 17102–17104.

[15] P. M. Allemand, A. Koch, F. Wudl, *J. Am. Chem. Soc.* **1991**, *113*, 1050–1051.

[16] T. F. Guarr, M. S. Meier, V. K. Vance, M. Klayton, *J. Am. Chem. Soc.* **1993**, *115*, 9862–9863.

[17] P. Boulas, F. D'Souza, C. C. Henderson, P. A. Cahill, M. T. Jones, K. M. Kadish, *J. Phys. Chem.* **1993**, *97*, 13435–13437.

[18] L. Echegoyen, L. E. Echegoyen, *Acc. Chem. Res.* **1998**, *31*, 593–601.

[19] A. J. Stone, D. J. Wales, *Chem. Phys. Lett.* **1986**, *128*, 501–503.

[20] a) S. J. Austin, P. W. Fowler, D. E. Manolopoulos, F. Zerbetto, *Chem. Phys. Lett.* **1995**, *235*, 146–151; b) H. F. Bettinger, B. I. Yakobson, G. E. Scuseria, *J. Am. Chem. Soc.* **2003**, *125*, 5572–5580.

[21] G. M. Sheldrick, *Acta Crystallogr. A* **2008**, *64*, 112–122.

Received: May 5, 2011
Published online: June 10, 2011

